D-3

LA-2277

LOS ALAMOS SCIENTIFIC LABORATORY

OF THE UNIVERSITY OF CALIFORNIA o LOS ALAMOS NEW MEXICO

A NUMERICAL SOLUTION OF A SPHERICAL BLAST WAVE UTILIZING A COMPLETELY TABULAR EQUATION OF STATE

LEGAL NOTICE

Printed in USA. Price $1.50 Available from the

Office of Technical Services
U. S. Department of Commerce
Washington 25, D. C.

LA-2277
PHYSICS AND MATHEMATICS
(TID-4500, 14th Ed.)

LOS ALAMOS SCIENTIFIC LABORATORY
OF THE UNIVERSITY OF CALIFORNIA LOS ALAMOS NEW MEXICO

REPORT WRITTEN: June 1958

REPORT DISTRIBUTED: June 15, 1959

A NUMERICAL SOLUTION OF A SPHERICAL BLAST WAVE UTILIZING A COMPLETELY TABULAR EQUATION OF STATE

by
Leland R. Stein

Contract W-7405-ENG. 36 with the U. S. Atomic Energy Commission

ABSTRACT

Using an equation of state of air in completely tabular form, a one dimensional, spherically symmetric blast wave calculation has been numerically carried out. An IBM 704 computer was utilized for the calculation. The Rankine-Hugoniot conditions at the shock front and the isentropic changes of the shocked fluid were determined by iterative methods. The numerical methods employed are discussed in some detail, as are the details of the equation of state. The initial starting conditions for this numerical integration were those of Problem M. The numerical results are presented in graphical form. Comparison to Problem M is also displayed graphically. The comparison to Problem M is good, the small differences being attributed to that of equation of state and finite differencing methods.

CONTENTS

FIGURES

1. INTRODUCTION

This work was undertaken in order to develop a sharp shock blast wave code. As a means of checking the present coding, Problem M,[1] a blast wave calculation for an energy release of 13.5 KT carried out at Los Alamos around 1945, was chosen as the comparison problem. The initial conditions of Problem M were used as the starting data for this code, thereby permitting each calculation cycle to be compared to those of Problem M. Such a comparison serves as a guide to determine if the present code is functioning properly, and if it is, serves also as a check on Problem M, for since the results of that problem have been used extensively, an independent comparative blast calculation is desirable. The results from this problem differ somewhat from those of Problem M, since the calculations for the latter were carried out on slow, semi-automatic equipment, with a substantial portion of M done by hand on desk calculators. Thus approximations consistent with realistic calculation times were necessary. In addition, a new equation of state for air[2,3,4] was used. Improvements in the numerical methods of Problem M were possible using the present day high speed, completely automatic computing machines.

The new equation of state data were in tabular form. Several exploratory attempts to find an analytic fit to these data indicated that a complex system of fits would undoubtedly be necessary. In general, since most analytic fits to equation of state data are poor except in

limited regions, and since the range of thermodynamic variables in blast problems is quite extreme, it was thought that if this new equation of state were used completely in tabular form, it would be more useful and accurate than an extremely complex system of fits. Given the relative specific volume and the specific internal energy, this tabular equation of state determines the pressure by a double interpolation of the tabular entries, or symbolically, $P = P(V/V_0, E)$. The details of the equation of state are discussed in Section 9.

The method used to determine the isentropic changes within the fluid of the shocked sphere is given in Sections 2 and 3.

The Rankine-Hugoniot conditions at the shock boundary are determined by an iterative method which is discussed in Section 4.

The addition of new fluid elements to the calculation is required as the shock discontinuity progresses further into the undisturbed fluid. This addition is considerably complicated by utilization of a "sharp shock" calculation[1,5,6] rather than a "smeared shock" calculation.[7,8,9] The addition procedure is explained in Section 5, and other fluid element adding schemes which were tried are described in Section 6.

The initial conditions chosen for this numerical integration represent the hydrodynamic state of an energy release of 13.2 KT at a time 12 milliseconds after detonation. There is a difference in total energy between this problem and that of Problem M because of the new equation of state used. Comparison values from the present problem and from Problem M are displayed graphically in Section 11.

2. THE BASIC EQUATIONS AND BOUNDARY CONDITIONS

We consider the region of a fluid bounded by a shock front. Within this bounded region the hydrodynamical state of the fluid is described by four equations: the equation of continuity, the equation of motion, the conservation of energy in the form of the first law of thermodynamics, and the equation of state. Spherical symmetry is assumed, and the Lagrangian form of the equation of motion is used. In the Lagrangian formulation we are concerned with the properties of fluid elements, which are tagged or identified by their initial positions, and we follow these elements along in space and time observing the changes of their fluid properties. Thus, the radius, pressure, density, velocity, internal energy, and acceleration of each fluid element are functions of the element's initial position and the time, or $R(r,t)$, $P(r,t)$, $\rho(r,t)$, $v(r,t)$, $E(r,t)$, and $a(r,t)$. R is referred to as the Eulerian radius and r as the Lagrangian radius, that is, R is the physical position of a fluid element at time t, and r is that element's initial position.

The equation of continuity or conservation of mass states that the initial mass of a specific fluid element remains in that element and there is no transport of mass from one element to another, or

$$\frac{\rho_0}{\rho} = \frac{V}{V_0} = \frac{\partial R^3}{\partial r^3}, \tag{2.1}$$

where V is the specific volume or the reciprocal of the density.

From Newton's second law the volume force is given by

$$\vec{F}_V = \rho \frac{\vec{dv}}{dt} = -\text{grad } P$$

and for spherical symmetry,

$$\frac{\partial v}{\partial t} = -\frac{1}{\rho} \frac{\partial P}{\partial R} . \tag{2.2}$$

Combining this with (2.1), we have

$$\frac{\partial v}{\partial t} = -\frac{1}{\rho_0} \frac{R^2}{r^2} \frac{\partial P}{\partial r} = -\frac{3R^2}{\rho_0} \frac{\partial P}{\partial r^3} . \tag{2.2'}$$

We require the changes of the fluid within the bounded volume to be isentropic, or

$$dE = -PdV. \tag{2.3}$$

The equation of state is in tabular form. The table is arranged so that for a given relative specific volume and specific internal energy the pressure is determined by a double interpolation scheme or, symbolically,

$$P = P\left(V/V_0, E\right). \tag{2.4}$$

See Section 9 for a more detailed discussion of the equation of state.

The above equations are valid behind the shock. At the shock, however, the equations of Rankine and Hugoniot are to be used. They are as follows:

$$\rho(u - \dot{\xi}) = \rho_0 \dot{\xi} \ , \tag{2.5}$$

$$\psi - P_0 = \rho_0 \dot{\xi} u \ , \tag{2.6}$$

$$E_\xi - E_0 = \tfrac{1}{2}(\psi + P_0)\left(1/\rho_0 - 1/\rho_\xi\right). \tag{2.7}$$

The material velocity of the unshocked region, u_0, is assumed to be zero. $\dot{\xi}$ is the shock velocity, u, the material velocity of the medium behind the shock, and ψ, the shock pressure.

There are two boundary conditions, one at the center of the disturbance, the other at the shock. They are as follows:

$$R(0,t) = 0 \quad \text{(for all t)} \tag{2.8}$$

and

$$R(\xi,t) = \xi \quad \text{(for all t)}, \tag{2.9}$$

where ξ is the Lagrangian radius of the shock front and is a function of time or $\xi = \xi(t)$. Equations (2.5), (2.6), (2.7), and (2.9) are not independent, as can be readily verified.

3. INTEGRATION OF THE BASIC EQUATIONS

The integration of the basic equations is carried out numerically in a stepwise manner. The differential equations are approximated by finite difference equations. In order to set up these difference

equations the bounded region is divided into finite regions or fluid elements of concentric spherical shells each of equal Lagrangian radial width. The radii bounding the elements are numbered consecutively outwards from the center, 0, 1, 2, 3, 4, $\cdots$, i-1, i, i+1, $\cdots$. The pressure, density, and internal energy of the entire element are considered to be that of the centroid of each fluid element but the acceleration and velocity are associated with the bounding radii. Let us consider the equations for a typical fluid element bounded by radii r_i and r_{i-1} at time t = n-1 and integrate these equations over a time interval Δt. We let the subscripts indicate the Lagrangian radii where the quantity is assumed located and the superscript, the time. Equation (2.2') then becomes

$$a_i^{n-1} = -\frac{6\left(R_i^{n-1}\right)^2}{\rho_0}\,\frac{P_{i+\frac{1}{2}}^{n-1} - P_{i-\frac{1}{2}}^{n-1}}{\Delta r_{i+\frac{1}{2}}^3 + \Delta r_{i-\frac{1}{2}}^3} = \frac{v^{n-\frac{1}{2}} - v^{n-3/2}}{\Delta t}\,, \qquad (3.1)$$

where $\Delta r_{i+\frac{1}{2}}^3 = (r_{i+1}^3 - r_i^3)$, and where an average of the two bounding Δr^3's is utilized for computational convenience. Solving for the velocity, we have

$$v_i^{n-\frac{1}{2}} = v_i^{n-3/2} + a_i^{n-1}\,\Delta t = \frac{R_i^n - R_i^{n-1}}{\Delta t}\,, \qquad (3.2)$$

and for the radius,

$$R_i^n = R_i^{n-1} + v^{n-\frac{1}{2}}\,\Delta t\,. \qquad (3.3)$$

Now, having the new outer radius of the element at t = n and assuming that we have previously, in a similar manner, determined the inner radius at t = n, we are in a position to determine the volume of the element at

time t = n.

$$\left(V/V_0\right)^n_{i-\frac{1}{2}} = \frac{1}{\Delta r^3_{i-\frac{1}{2}}}\left[\left(R^n_i\right)^3 - \left(R^n_{i-1}\right)^3\right]$$

$$= \frac{1}{\Delta r^3_{i-\frac{1}{2}}}\left\{\left(R^n_i - R^n_{i-1}\right)\left[\left(R^n_i\right)^2 + R^n_{i-1}\left(R^n_i + R^n_{i-1}\right)\right]\right\}. \qquad (3.4)$$

Equations (2.3) and (2.4) in difference form become

$$E^n_{i-\frac{1}{2}} = E^{n-1}_{i-\frac{1}{2}} - \frac{\left(P^n_{i+\frac{1}{2}} + P^n_{i-\frac{1}{2}}\right)}{2\rho_0}\left[\left(V/V_0\right)^n_{i-\frac{1}{2}} - \left(V/V_0\right)^{n-1}_{i-\frac{1}{2}}\right] \qquad (3.5)$$

and

$$P = P\left(V/V_0,\ E\right). \qquad (3.6)$$

Assuming that we know all the above quantities except $P^n_{i-\frac{1}{2}}$ and $E^n_{i-\frac{1}{2}}$ and have determined the volume of this element at time t = n-1, we can solve Equations (3.5) and (3.6) simultaneously by iteration.

We have demonstrated how a typical element is integrated from time t = n-1 to t = n; this process is carried out for each element starting from the center and working toward the shock front. The last element, however, needs to be treated differently, as there is no Δr^3 conveniently available. The acceleration is formed as follows:

$$a^{n-1}_I = -\frac{2}{\rho_0}\frac{\left(R^n_I\right)^2\left(\psi^{n-1} - P^{n-1}_{I-\frac{1}{2}}\right)}{r^2_I\left(2\xi - r_I - r_{I-1}\right)}. \qquad (3.7)$$

The subscript I indicates the element adjacent to the shock. After carrying out the above scheme we have all the information required within the bounded region. We now determine the shock quantities.

4. DETERMINATION OF THE SHOCK QUANTITIES, OR THE SHOCK FITTING

The method used to determine the shock conditions is discussed in LA-1148 (Ref. 5) and is an iterative scheme. We briefly outline it here as follows: One guesses a shock volume ${}_{g}V_{\xi} = V_{\xi}/V_0$ (the reciprocal of the shock compression). From the simultaneous solution of Equations (2.4) and (2.7) (an iterative process), the values of ψ, E_{ξ}, and $\frac{d\psi}{dV_{\xi}} = -S$ of the Hugoniot are determined. The shock velocity is

$$\dot{\xi}^n = \sqrt{V_0}\, W^n, \tag{4.1}$$

where $(W^n)^2 = \frac{\psi - P_0}{1 - {}_{g}V_{\xi}}$. The position of the shock is determined at time $t = n$ by

$$\xi^n = \xi^{n-1} + \frac{\Delta t}{2}\left(\dot{\xi}^n + \dot{\xi}^{n-1}\right). \tag{4.2}$$

Using the relation for the total time derivative of the shock volume in terms of the above determined quantities, we have

$$\dot{V}_{\xi} = \frac{d}{dt}\left(\frac{V}{V_0}\right)_{\xi} = 2\dot{\xi}/(3W^2 + S)\left[\frac{2V_{\xi}\psi}{\xi} + \left(\frac{\partial P}{\partial r}\right)_{\xi} + W^2\left(\frac{\partial V}{\partial r}\right)_{\xi}\right] \tag{4.3}$$

and in difference form,

$$\left(\frac{dV_\xi}{dt}\right)^n = \dot{V}_\xi^n = \frac{4\dot{\xi}^n}{3(W^n)^2 + S^n}\left[\frac{V_\xi^n(\psi - P_0)}{\xi^n} + \frac{(W^n)^2\left(1 - V_{I-\frac{1}{2}}^n\right) + P_0 - P_{I-\frac{1}{2}}^n}{2\xi^n - r_i - r_{i-1}}\right]. \quad (4.3')$$

From the above $\dot{V}_\xi^n$ and the value at n-1 we can determine an average change in the shock volume in the time interval Δt. Adding this to V_ξ^{n-1}, we have a calculated volume ${}_cV_\xi^n$, or

$$\Delta V^{n-\frac{1}{2}} = \frac{\Delta t}{2}\left(\dot{V}_\xi^n + \dot{V}_\xi^{n-1}\right) \quad (4.4)$$

$${}_cV_\xi^n = V_\xi^{n-1} + \Delta V_\xi^{n-\frac{1}{2}} . \quad (4.5)$$

Comparison of ${}_gV_\xi^n$ and ${}_cV_\xi^n$ determines whether the iteration is completed. If it is not, a new guess is carried out based on previous guesses. When the "shock fitting" is completed, the integration of all the equations from time $t = n-1$ to time $t = n$ has been completed. Integration from time $t = n$ to time $t = n+1$, etc., is carried out by repeating the steps of Sections 3 and 4. However, when the shock position ξ becomes greater than $r_I + \Delta r = r_{I+1}$, a new fluid element must be added to the calculation.

5. ADDING A NEW FLUID ELEMENT

In order to add a fluid element, or mass point, one needs to obtain values of the pressure, volume, internal energy, velocity, and the radius at the appropriate Lagrangian radii and times, i.e., we need

$P_{I+\frac{1}{2}}^n$, $V_{I+\frac{1}{2}}^n$, $E_{I+\frac{1}{2}}^n$, $v_{I+1}^{n-\frac{1}{2}}$, and R_{I+1}^n. Since the shock fitting is dependent

upon the pressure and volume gradients behind the shock front [cf. (4.3)], the new fluid element values and the shock quantities are determined simultaneously by an iteration scheme. Thus during the course of a shock fitting when the results of Equation (4.2) indicate that $\xi^n \geq r_I + \Delta r \equiv r_{I+1}$, the normal shock fitting scheme is interrupted and the above mentioned values of the new fluid element are created in a method consistent with ${}_gV_\xi$. (This method is discussed in more detail later in this section.) The shock fitting is then continued at (4.3), using now, however, the pressure and volume just created. If the comparison of ${}_gV_\xi$ and ${}_cV_\xi$ is not satisfactory, a new ${}_gV_\xi$ is made and the mass point adding, shock fitting iteration is continued. The creation of the new element values is carried out on each of these iteration cycles. This iteration scheme is continued until ${}_gV_\xi$ and ${}_cV_\xi$ agree to the desired accuracy. The interruption of the shock fitting scheme is made only on the intergration cycle when $\xi^n \geq r_I + \Delta r \equiv r_{I+1}$. After the new fluid element is added, the interruption of the shock fitting scheme stops and the calculation continues in its normal manner, except that there is one more mass point, until it is again determined by (4.2) that another element needs to be added.

The quantities of interest for the new fluid element are created by the following method. First, the time at which the shock position equals $r_I + \Delta r \equiv r_{I+1}$ is determined.

Let

$$t_1 = \frac{r_{I+1} - \xi^{n-1}}{\dot{\xi}^{n-1}} \qquad \text{and} \qquad t_2 = \frac{\xi^n - r_{I+1}}{\dot{\xi}^n} .$$

In general, since $t_1 + t_2 \neq \Delta t$, a weighted average of t_1 and t_2 is used to describe the time of crossing. This time becomes $t^* = t^{n-1} + T_1$, where

$$T_1 = \frac{t_1}{\Delta t} (2\Delta t - t_1 - t_2). \tag{5.1}$$

We also designate T_2 such that $T_2 = \Delta t - T_1$. For convenience we indicate by I the fluid element being added. The quantities of interest for the new mass point at the time $t = t^*$ are now determined. The radius is

$$R_I^* = r_I = \xi^* . \tag{5.2}$$

The shock volume at this time, $t = t^*$, is determined by

$$V_\xi^* = \frac{1}{\Delta t} (T_2 V_\xi^{n-1} + T_1 V_\xi^n). \tag{5.3}$$

Using V_ξ^*, we next solve Equations (2.7) and (2.4) for E_ξ^* and ψ_ξ^*. The inner bounding radius is determined at time $t = t^*$ by

$$R_{I-1}^* = R_{I-1}^n - v_{I-1}^{n-\frac{1}{2}} T_2, \tag{5.4}$$

and the volume at time $t = t^*$ is

$$V_{I-\frac{1}{2}}^* = \frac{1}{\Delta r_{I-\frac{1}{2}}^3} \left(r_I - R_{I-1}^*\right)\left[r_I^2 + R_{I-1}^* \left(R_{I-1}^* + r_I\right)\right]. \tag{5.5}$$

The internal energy at time t = t* is obtained by a three point interpolation, or

$$E^*_{I-\frac{1}{2}} = 0.533\, E^*_{\xi} + 0.667\, E^*_{I-3/2} - 0.200\, E^*_{I-5/2}, \tag{5.6}$$

where $E^*_{I-3/2}$ and $E^*_{I-5/2}$ are determined by interpolation from values at times t = n and t = n-1. $P^*_{I-\frac{1}{2}}$ is obtained through the equation of state (2.4) since $V^*_{I-\frac{1}{2}}$ and $E^*_{I-\frac{1}{2}}$ are now known. The velocity of the new mass point at t = t* is the material velocity of the shock, or

$$v^*_I = \left[V_0\left(\psi^* - P_0\right)\left(1 - V^*_{\xi}\right)\right]^{\frac{1}{2}}. \tag{5.7}$$

We now know all the necessary quantities of the new mass point at t = t*; however, in order that they will fit into the general differencing scheme it is necessary to advance them to their proper times. First we determine R^n_I, $v^{n-\frac{1}{2}}_I$, and $V^n_{I-\frac{1}{2}}$.

$$R^n_I = R^{n-1}_I + v^{n-\frac{1}{2}}_I \Delta t, \tag{5.8}$$

where

$$R^{n-1}_I = r_I - v^*_I T_1 + \tfrac{1}{2} a^*_I T_1^2, \tag{5.9}$$

$$v^{n-\frac{1}{2}}_I = v^*_I + \frac{a^*_I}{2}\left(T_2 - T_1\right), \tag{5.10}$$

and

$$a^*_I = -\frac{\psi^* - P^*_{I-\frac{1}{2}}}{\rho_0 \frac{\Delta r}{2}}. \tag{5.11}$$

The volume of the new element is then at $t = t^n$

$$V^n_{I-\frac{1}{2}} = \frac{1}{\Delta r^3_{I-\frac{1}{2}}} \left\{ \left(R^n_I - R^n_{I-1} \right) \left[\left(R^n_I \right)^2 + R^n_{I-1} \left(R^n_I + R^n_{I-1} \right) \right] \right\} \quad (5.12)$$

Since we have $P^*_{I-\frac{1}{2}}$, $E^*_{I-\frac{1}{2}}$, $V^*_{I-\frac{1}{2}}$, and $V^n_{I-\frac{1}{2}}$, we can solve Equations (3.5) and (3.6) for the values of $P^n_{I-\frac{1}{2}}$ and $E^n_{I-\frac{1}{2}}$, that is, we require the newly formed element to change isentropically from $t = t^*$ to $t = t^n$. We now have all the necessary quantities for the new point.

6. OTHER ELEMENT ADDING SCHEMES

Several other schemes were tried in order to add the new fluid element; however, that of Section 5 proved to be the most satisfactory in regards to smoothness of the P, V, E, v, and R profiles at the time of adding, and particularly in regards to the conservation of total energy.

The other methods are now briefly discussed. The determination of t^* is the same for all the methods tried and is that described by Equation (5.1).

a. Use of the Shock Quantites at Times t^* and t^{*-1}

Equations (5.8) - (5.12) were used to determine R^n_I, $v^{n-\frac{1}{2}}_I$, and $V^n_{I-\frac{1}{2}}$ with, however, the exception that a^{n-1}_{I-1} was used for a^*_I. Having the shock quantities at the present * time t^* and at the previous * time t^{*-1}, the assumption is made that the internal energy of the new element at time $t = t^n$ is the average of these shock internal energies. Then $P^n_{I-\frac{1}{2}}$ is determined by the equation of state (2.4).

This method produced relatively smooth profiles at the time of adding; however, the conservation of the total energy of the problem was not so good as that of the method of Section 5.

b. Original point on the Hugoniot

Using the scheme of 6a to determine R_I^n, $v_I^{n-\frac{1}{2}}$, and $V_{I-\frac{1}{2}}^n$, a point on the Hugoniot between time t^* and time t^{*-1} is chosen as representative of the entire new element. We follow along the adiabat or expand the new element isentropically to the volume $V_{I-\frac{1}{2}}^n$. In this manner we determine the pressure $P_{I-\frac{1}{2}}^n$ and the internal energy $E_{I-\frac{1}{2}}^n$ at time $t = t^n$. The representative point chosen was the point corresponding to the shock quantities as the shock crossed the centroid of the new element. The results proved to be poor, and changing the representative point brought little improvement. This scheme, though physically real, is not consistent with the differencing scheme. This is clear if one considers the region between the shock and the last mass point. This region is not carried (in this problem) in the regular advancing scheme until the new point is added, i.e., the differencing scheme of this small region considers that only the region possesses mass. The energy, pressure, etc., are ignored until the new mass point is added, and only then are the isentropic changes carried. Thus this method is not appropriate for our present differencing scheme.

Carrying the region between the shock and the last mass point as a regular mass point, that is, considering isentropic changes, would be advantageous; however, the special calculations involved make it cumbersome to handle such a calculation for the numerical integration.

c. v_I^* Variation

Since it can be argued that one really needs an average velocity for the differencing scheme and not the bounding value, v_I^* was varied in schemes a and b by utilizing various space weighting factors. Although this method was effective in changing the newly added values to adjust smoothly in specific cases, it was not possible to find a weighting scheme which would be satisfactory for all cases.

d. Gradient as Three Point Fits

In the shock fitting scheme of Section 4, $\dot{V}_\xi$ depends on $\left(\frac{\partial V}{\partial r}\right)_\xi$ and $\left(\frac{\partial P}{\partial r}\right)_\xi$ (see 4.3). Equation (4.3') uses a two point difference as the approximation to the derivative. A three point fit was carried out for both V(r) and P(r) and the derivative evaluated at r = ξ determined. These values were then substituted in (4.3) and the shock fitting scheme used this value of $\dot{V}_\xi$. This scheme functioned nicely on regular cycles; however, on the add mass point cycles the values of ${}_gV_\xi$ and ${}_cV_\xi$ would agree to only about 5 per cent. The pressure gradient used in the last mass point acceleration term was also determined by a three point fit of P(r); i.e., $\left(\frac{\partial P}{\partial r}\right)_I$ from the fit was used in Equation (3.7). This too had no appreciable effect and did not help the poor convergence described above.

e. No Coupling in the Point Add Scheme

In this scheme the shock properties and the new point quantities were not determined simultaneously. The new point quantities were determined after the shock fitting; however, the same methods outlined in

Section 5 for the point adding were still used. This method though good was not so good as that of the simultaneously determined method of Section 5.

f. Variation of the Time Interval Δt

It was found that even though the stability conditions were good, the new mass point data could be improved if the time interval Δt was reduced.

g. Combinations of the Above Schemes

Several combinations of the above schemes were tried. For example, schemes a and e were tried, also schemes a, c, and e; or the scheme of Section 5 with those of e and/or c, etc.

After trying a number of these combinations, the method of Section 5 proved to be the best.

7. STABILITY CHECKS

The Courant stability condition was employed in order to ensure a stable differencing scheme. A stability number was calculated for each mass point every integration cycle. If the stability number exceeded a particular value, Δt of the next calculating cycles was reduced by a factor of 2. Similarly, if the stability number remained below another particular value for several calculation cycles, the Δt of the next calculation cycles could be increased by a factor of 2. The problem was automatically monitored for the stability time halving, but that for the time doubling was carried out visually by the operator. The

approximate difference form of the stability relation used was

$$L^{n}_{i-\frac{1}{2}} = \frac{\sqrt{\gamma/\rho_0}\sqrt{P^{n}_{i-\frac{1}{2}}V^{n}_{i-\frac{1}{2}}}\Delta t}{R^{n}_{i} - R^{n}_{i-1}} . \tag{7.1}$$

In (7.1), the sound velocity was approximated by that of an ideal gas with $\gamma = 1.4$. The maximum stability number and its corresponding mass point number were stored each integration cycle and printed as so desired.

8. ENERGY CALCULATIONS

The total energy of the problem was calculated every integration cycle; however, the energy calculated on cycle n was the energy for cycle n-1, the reason being that the velocity is centered in time at $n-\frac{1}{2}$.

The kinetic energy of each mass point was computed as follows:

$$\left(\text{K.E.}\right)^{n-1}_{i-\frac{1}{2}} = \tfrac{1}{2}M_{i-\frac{1}{2}}\left(v^{n-1}_{i-\frac{1}{2}}\right)^2 , \tag{8.1}$$

where $M_{i-\frac{1}{2}} = 4/3\pi\rho_0\Delta r^{3}_{i-\frac{1}{2}}$ (the mass of the element) and where

$$v^{n-1}_{i-\frac{1}{2}} = \tfrac{1}{2}\left[\left(v^{n-1}_{i}\right)^2 + \left(v^{n-1}_{i-1}\right)^2\right] ,$$

with

$$v^{n-1}_{i} = \frac{v^{n-\frac{1}{2}}_{i} + v^{n-3/2}_{i}}{2} .$$

The internal energy of a mass point was calculated simply as

$$U^{n-1}_{i-\frac{1}{2}} = E^{n-1}_{i-\frac{1}{2}} M_{i-\frac{1}{2}} . \tag{8.2}$$

The energy within the small region between the shock and the last mass point is obtained by interpolation. The kinetic energy is

$$\left(\text{K.E.}\right)^{n-1}_{\xi-\frac{1}{2}} = \tfrac{1}{2}\left(v^{n-1}_{\xi-\frac{1}{2}}\right)^2 M_{\xi-\frac{1}{2}}, \tag{8.3}$$

where

$$\left(v^{n-1}_{\xi-\frac{1}{2}}\right)^2 = \frac{\left(v^{n-1}_{I}\right)^2 + \left[\dot{\xi}^{n-1}\left(1 - V^{n-1}_{\xi}\right)\right]^2}{2}$$

and $$v^{n-1}_{I} = \frac{v^{n-\frac{1}{2}}_{I} + v^{n-3/2}_{I}}{2},$$

and where

$$M^{n-1}_{\xi-\frac{1}{2}} = 4/3\pi\rho_0 \left(\xi^{n-1} - r_I\right)\left[\left(\xi^{n-1}\right)^2 + r_I\left(\xi^{n-1} + r_I\right)\right].$$

The internal energy is

$$U^{n-1}_{\xi-\frac{1}{2}} = E^{n-1}_{\xi-\frac{1}{2}} M_{\xi-\frac{1}{2}}, \tag{8.4}$$

where

$$E^{n-1}_{\xi-\frac{1}{2}} = E^{n-1}_{\xi} + \left(\frac{E^{n-1}_{\xi} - E^{n-1}_{I-\frac{1}{2}}}{\xi^{n-1} - \dfrac{R^{n-1}_{I} + R^{n-1}_{I-1}}{2}}\right)\left(\xi^{n-1} - \frac{\xi^{n-1} + R^{n-1}_{I}}{2}\right).$$

The total kinetic energy is then the sum of all these elemental kinetic energies, or

$$(\text{K.E.})^{n-1} = (\text{K.E.})^{n-1}_{\xi-\frac{1}{2}} + \sum_{i=1}^{I} (\text{K.E.})^{n-1}_{i-\frac{1}{2}}. \tag{8.5}$$

Summing over all the elemental internal energies also gives the total internal energy; however, the ambient internal energy of the medium must first be subtracted.

$$(U)^{n-1} = U_{\xi-\frac{1}{2}}^{n-1} + \sum_{i=1}^{I} U_{i-\frac{1}{2}}^{n-1} - 4/3\,\dot{\pi}\rho_0 E_0\left[\left(\xi^{n-1}\right)^3 - \xi_0^3\right]. \quad (8.6)$$

The total energy of the problem is then

$$\mathcal{E}^{n-1} = (\text{K.E.})^{n-1} + (U)^{n-1}. \quad (8.7)$$

Figures 13, 14, and 15 show the total energy, the total internal energy, and the total kinetic energy, respectively, plotted as functions of the time.

9. THE EQUATION OF STATE OF AIR

The equation of state is in tabular form. The pressure is determined as a function of the specific energy and the relative specific volume through the table searching, double-quadratic, interpolating subroutine 1-B and a table of thermodynamic values. This table is composed for specific values of $\log_{10}(V/V_0)$ and corresponding to each is a set of values of PV and E. There are 15 $\log_{10}(V/V_0)$ values ranging in 0.2 intervals from -1.2 to +1.6. For each $\log_{10}(V/V_0)$ there are 61 sets of PV, E values. Each set of PV, E corresponds to a specific temperature, thus 61 temperatures are represented. These temperatures range in value from 200°K to $2{,}512{,}000^{\circ}$K.

The basic data sources for the table were References 2, 3, 4, and 10. The temperature range is divided into three parts: low, intermediate, and high. Reference 2 was the source for values in the low temperature range ($200^{\circ}K$ - $1900^{\circ}K$). As these data were in quite a different form from that desired, it was necessary to interpolate the data and rearrange it to conform with the above chosen tabular form. Reference 3 was the source for the intermediate range values ($2000^{\circ}K$ - $15{,}000^{\circ}K$). Values in the high temperature range ($15{,}950^{\circ}K$ - $2{,}512{,}000^{\circ}K$) were taken from Reference 4. Here again, the data were not in the desired form and interpolation was required. The contribution of radiant energy to these thermodynamic values was added using the relation

$$E_r = \frac{8}{15}\pi^5 \frac{K^4}{(hc)^3}\frac{T^4}{\rho} = \frac{aT^4}{\rho}, \tag{9.1}$$

where a is the radiation density constant

$$(PV)_r = 1/3E_r. \tag{9.2}$$

After these processes were carried out for the high temperature range, Reference 10 became available. Comparison of the values in Reference 10 with the above interpolated ones proved quite good, and the high temperature range values were therefore not changed. As each of these references assumes somewhat different models for the basic constituents of the air gas, it is not surprising to find that in the regions of overlapping there was some disagreement. Although the disagreements were small, their manifestations in the iterative schemes were acute. The thermo-

dynamic functions in the region of overlapping were then plotted and so adjusted as to form a continuous fit. The final tabular internal energy values are based on the ground state of the molecule.

The $\log_{10}(V/V_0)$ values in the table are normalized to the air model of Reference 3 at standard conditions. By changing the initial density constant in sub-routine 1B, the normalization of the table is effectively changed to that of any initial density within the limits of the tabular data.

The sub-routine functions as follows (see Figure 1): Given a value of V/V_0 (normalized to the table) and E, the sub-routine searches the table values of $\log_{10}(V/V_0)$ and finds the three nearest ones. This effectively locates the three bracketing sets of PV, E values of constant $\log_{10}(V/V_0)$ or, let us say, curves 1, 2, and 3. Having found these bracketing curves, it then searches the sets of PV, E values of each bracketing curve for the three PV, E sets nearest the given value of E. It then quadratically interpolates, for each curve, the three PV, E values for the value of PV corresponding to the given E. Finally, it quadratically interpolates the three above determined PV values and their corresponding $\log_{10}(V/V_0)$ values for the PV corresponding to the given V/V_0. The pressure is then obtained from this PV value, since V is known.

10. INITIAL CONDITIONS (STARTING DATA)

The initial conditions for this integration were chosen to be those of Problem M (see LA-2000, Chapter 6, Section 6.2). These conditions were prepared by J. Hirschfelder and J. Magee and represent the

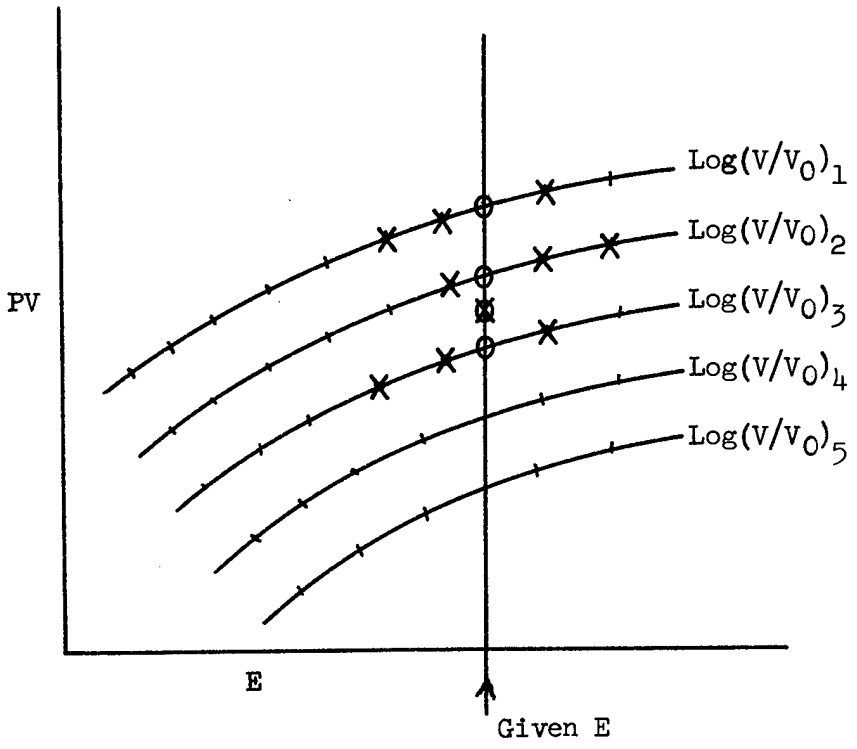

Fig. 1. Schematic diagram of double quadratic interpolation
X nearest points on bracketing curves

O interpolated PV values corresponding to given E for each bracketing curve

⊠ interpolated value corresponding to given E and given V/V_0

hydrodynamic state of a 13.5 KT explosion 12 milliseconds after detonation. Radiation transport was considered in the determination of the fire ball developmental stages. The pressures, velocities, radii, and volumes of Problem M were used directly; however, the internal energies were determined from the present equation of state using the given pressures and volumes. This was necessary in order to maintain a pressure, a volume, and an internal energy consistent with this equation of state. Similarly the shock pressure of Problem M was used directly and, from the Hugoniot conditions, using this shock pressure, the shock volume and energy were determined.

These initial data are:

Undisturbed Medium

$\rho_0 = 1.1613 \times 10^{-3}$ gm/cm^3 $\quad P_0 = 1 \times 10^6$ dynes/cm^2 $\quad E_0 = 2.1421 \times 10^9$ ergs/gm

Shock Quantities

$\psi = 7.7246 \times 10^7$ dynes/cm^2 $\quad V_\xi = 1.3860$ $\quad E = 3.1162 \times 10^{10}$ ergs/gm

$\xi = 7.9879 \times 10$ meters $\quad \dot{\xi} = 2.7608$ meters/millisec

$\dot{V}_\xi = 2.7253 \times 10^{-3}$/sec

Regular Mass Points

Initially there were 16 mass points. The isothermal sphere is contained between the center and mass point 1.

$\Delta r = 3.994$ meters $\quad \Delta t = 6.25 \times 10^{-2}$ millisec

Mass Point	$P^n_{i-\frac{1}{2}}$	$E^n_{i-\frac{1}{2}}$	$R^n_{i-\frac{1}{2}}$	$v^{n-\frac{1}{2}}_i$	$V^n_{i-\frac{1}{2}}$
1	3.6986×10^{7}	4.9686×10^{12}	6.0232×10	1.4586×10	2.7437×10
2	3.7253×10^{7}	7.3494×10^{11}	6.2167×10	1.5376×10	3.7513×10
3	3.7897×10^{7}	5.5993×10^{11}	6.4075×10	1.6136×10	2.8183×10
4	3.8783×10^{7}	4.5551×10^{11}	6.5918×10	1.6894×10	2.1699×10
5	3.9883×10^{7}	3.8328×10^{11}	6.7675×10	1.7634×10	1.7011×10
6	4.1245×10^{7}	3.1181×10^{11}	6.9335×10	1.8350×10	1.3530×10
7	4.2903×10^{7}	2.4622×10^{11}	7.0886×10	1.9051×10	1.0852×10
8	4.4864×10^{7}	1.9120×10^{11}	7.2325×10	1.9712×10	8.7468×10^{-1}
9	4.7147×10^{7}	1.4807×10^{11}	7.3646×10	2.0348×10	7.0673×10^{-1}
10	4.9800×10^{7}	1.1619×10^{11}	7.4847×10	2.0945×10	5.6983×10^{-1}
11	5.2825×10^{7}	9.5871×10^{10}	7.5942×10	2.1512×10	4.6437×10^{-1}
12	5.6250×10^{7}	8.1430×10^{10}	7.6934×10	2.2045×10	3.7873×10^{-1}
13	6.0110×10^{7}	6.7938×10^{10}	7.7817×10	2.2557×10	3.0447×10^{-1}
14	6.4378×10^{7}	5.5449×10^{10}	7.8598×10	2.3018×10	2.4488×10^{-1}
15	6.9123×10^{7}	4.4289×10^{10}	7.9284×10	2.3441×10	1.9605×10^{-1}
16	7.4391×10^{7}	3.5017×10^{10}	7.9879×10	2.3823×10	1.5558×10^{-1}

These data are identical to Problem M starting data except for the change to a new equation of state, which changes the total energy to 13.2 KT; also, Δt is one-fourth that of Problem M, and there are corresponding changes in the velocity at $n-\frac{1}{2}$.

11. RESULTS AND COMPARISON TO PROBLEM M

The results of this integration are presented in graphical form in Figures 2-16. Comparison to Problem M is also shown. The integration of the present problem was carried out to a shock overpressure of about 3 atmospheres, corresponding approximately to a shock radius of 350 meters and an elapsed calculation time of 300 milliseconds or 312 milliseconds after detonation. The calculation was not carried further, however, as the large amount of machine time required indicated a need for a logistical change in this problem. The time difficulty arose not through the use of the tabular equation of state, but through the ever increasing number of mass points added to the calculation as the shock progressed. It is believed that if the methods of H. H. Goldstine and J. von Neumann[6] were employed, this difficulty would be alleviated.

The comparison to Problem M is quite good, as the comparative figures indicate. The small differences in the comparative plots are due primarily to the differences in the equations of state used. Also, the method of adding new fluid elements contributes to some of this difference (see Figure 16). The number heading each adiabat in Figure 16 refers to the fluid element followed. Initially, since there are 16 fluid

elements, the pressure-volume point heading the adiabats are identical; however, the pressure-volume points of the newly added points (17, etc.) do not agree because of the difference in the adding schemes.

Since it would be extremely tedious to compute the energy of Problem M for each integration cycle, no comparative plot is made in Figures 13, 14, and 15. The initial nonsmoothness of the internal energy curve can be attributed to the two point interpolation scheme used for the energy calculation in the region between the shock and the last mass point. Although the starting data of Problem M had an energy content of 13.5 KT, that of the present problem contained 13.2 KT. Again this difference is due to the equation of state differences. The positive change in the total energy from the first integration cycle to the last, representing about 1400 integration cycles, was 0.66 per cent. The total energy of Problem M, with the shock front located at 2000 meters, is 13.1 KT, representing a 3 per cent loss.

REFERENCES

1. H. A. Bethe et al., Blast Wave, Los Alamos Scientific Laboratory Reports LA-1021 (August 1947) (classified) and LA-2000 (August 1947).

2. J. Hilsenrath et al., Tables of Thermal Properties of Gases, National Bureau of Standards Circular 564, U. S. Government Printing Office, Washington, D. C., 1955.

3. J. Hilsenrath and C. W. Beckett, Tables of Thermodynamic Properties of Argon-Free Air to 15,000°K, Report AEDC-TN-56-12 (September 1956), ASTIA Document No. AD-98974, U. S. Air Force, Arnold Development Center, Tullahoma, Tenn.

4. J. E. Weidenborner, Thermodynamic Properties of Air at High Temperatures, Report AFSWC-TN-56-48 (December 1956), U. S. Air Force Special Weapons Center, Albuquerque, N. M.

5. G. N. White, Jr., Hydrodynamic and Shock Relations for Problems with Spherical and Cylindrical Symmetry, Los Alamos Scientific Laboratory Report LA-1148 (August 1950) (classified).

6. H. H. Goldstine and J. von Neumann, Blast Wave Calculation, Communs. Pure and Appl. Math., 8, 327 (1955).

7. J. von Neumann and R. D. Richtmyer, A Method for the Numerical Calculation of Hydrodynamic Shocks, J. Appl. Phys., 21, 232 (1950).

8. H. L. Brode, Numerical Solutions of Spherical Blast Waves, J. Appl. Phys., 26, 766 (1955).

9. R. Latter, Similarity Solution for a Spherical Shock Wave, J. Appl. Phys., 26, 954 (1955).

10. J. Hilsenrath et al., Thermodynamic Properties of Highly Ionized Air, Report AFSWC-TR-56-35 (April 1957), ASTIA Document No. AD-96303, U. S. Air Force Special Weapons Center, Albuquerque, N. M.

BIBLIOGRAPHY

1. H. L. Brode, Point Source Explosion in Air, Rand Corporation Report RM-1824-AEC (December 1956).

2. R. H. Cole, Underwater Explosions, Princeton University Press, Princeton N. J., 1948.

3. R. Courant and K. O. Friedrichs, Supersonic Flow and Shock Waves, Interscience Publishers, New York, N. Y., 1956.

4. C. F. Curtiss and J. O. Hirschfelder, Thermodynamic Properties of Air, Report CM-472 (June 1948), University of Wisconsin Naval Research Laboratory, Madison, Wis.

5. H. K. Dasgupta and W. G. Penney, Pressure-Time Curves for Submarine Explosions, British Report BM-100 (July 1942).

6. F. R. Gilmore, Equilibrium Composition and Thermodynamic Properties of Air to 24,000°K, Rand Corporation Report RM-1543 (August 1955).

7. J. O. Hirschfelder and C. F. Curtiss, Thermodynamic Properties of Air II, Report CM-518 (December 1948), University of Wisconsin Naval Research Laboratory, Madison, Wis.

8. H. C. Kranzer, Shock Waves Produced by Nuclear Explosions at High Altitudes, internal Los Alamos Group Report J-10-336.

9. W. G. Penney, The Pressure-Time Curve for Underwater Explosions, British Report BM-99 (November 1940).

10. M. H. Rogers, Analytic Solutions for the Blast Wave Problem with an Atmosphere of Varying Density, Astrophys. J., 125, 478 (1957).

11. G. I. Taylor, The Formation of a Blast Wave by a Very Intense Explosion. I. Theoretical Discussion, Proc. Roy. Soc. (London), A201, 159 (1950).

12. J. D. Thomas, Present Status of the Problem of Computing the Propagation of a Strong Shock Wave in Air, internal Los Alamos Group Report J-10-292.

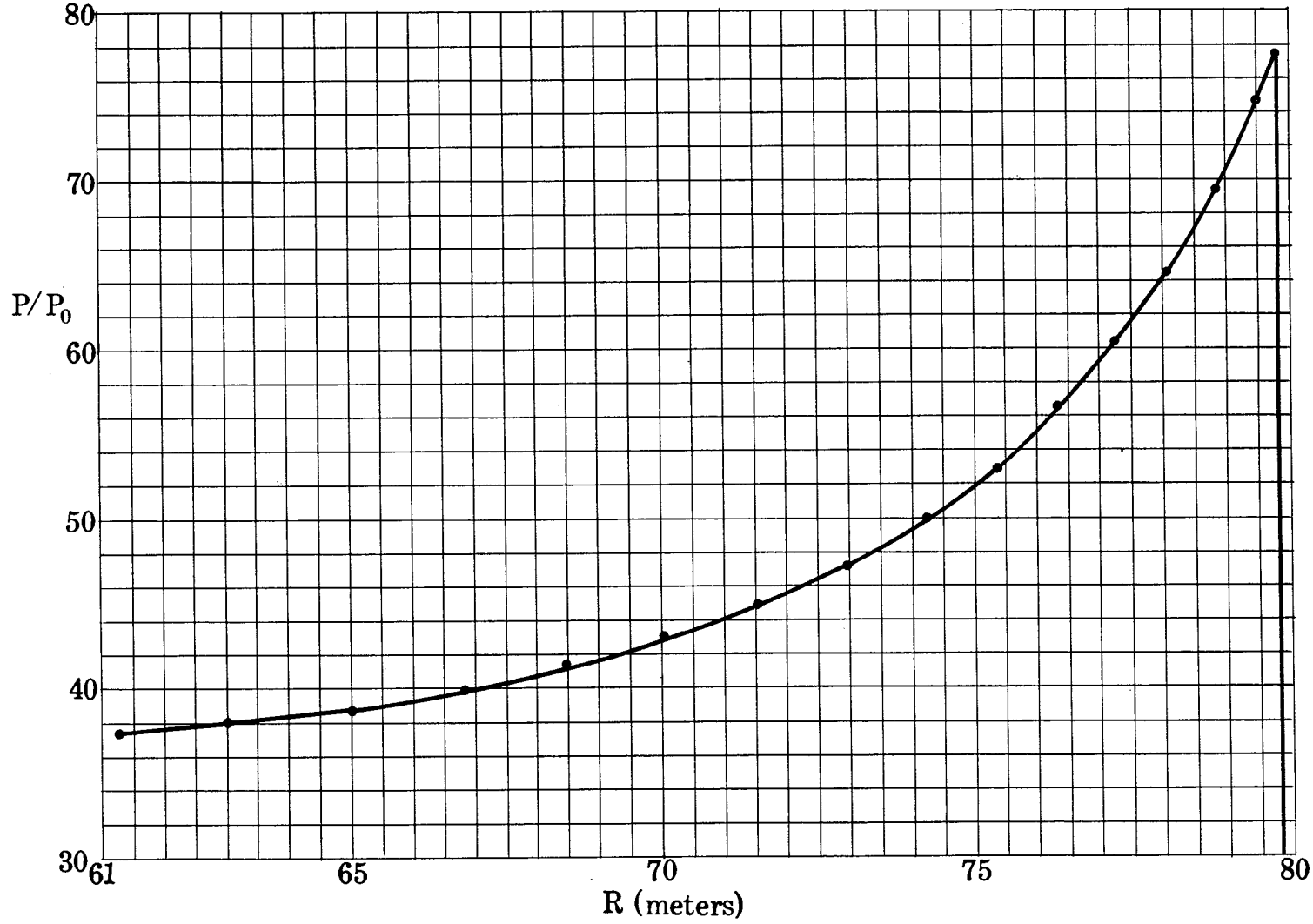

Fig. 2. Pressure as a function of the Eulerian radius at t = 0 milliseconds for both Problem M and Problem Herman

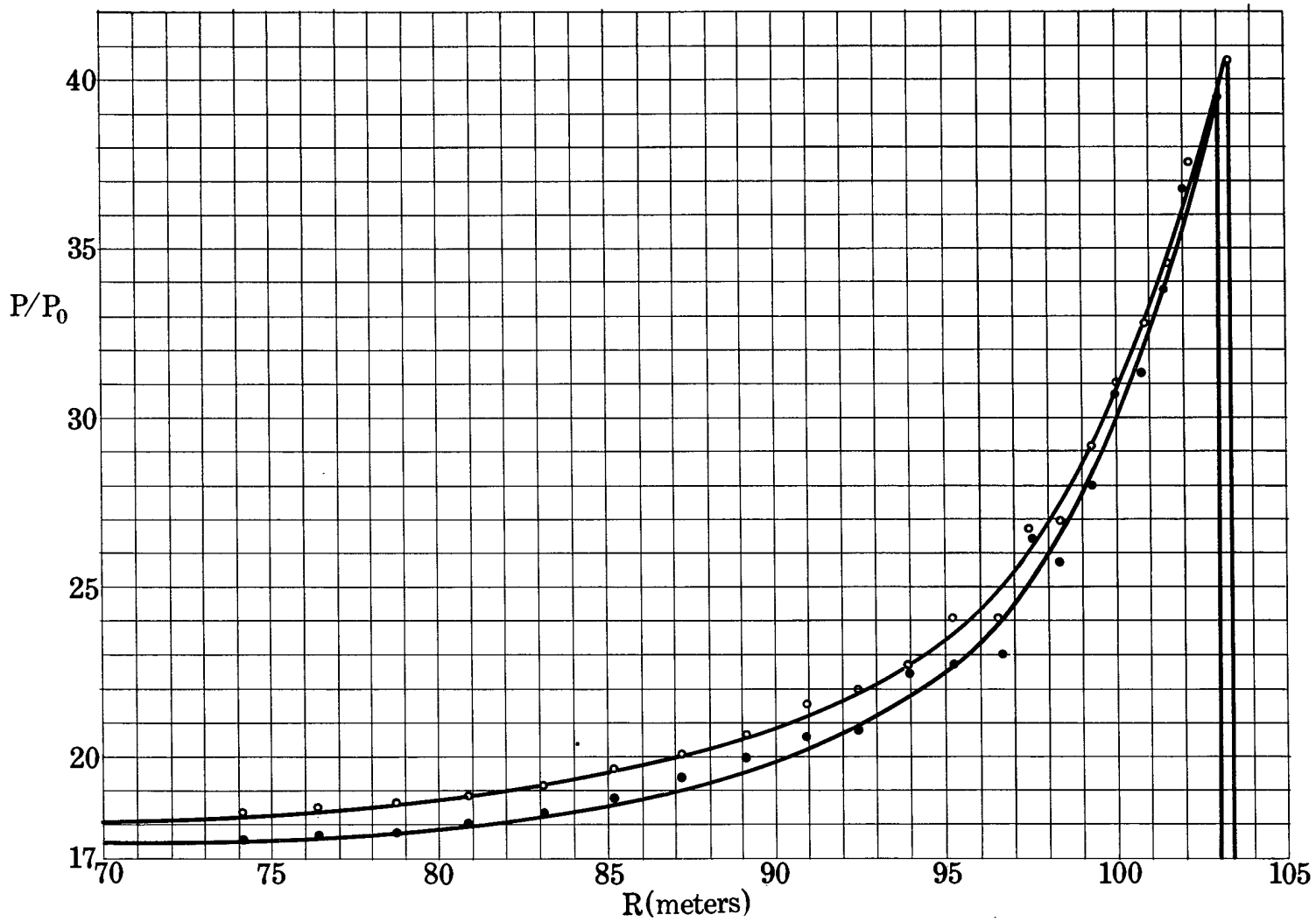

Fig. 3. Pressure as a function of the Eulerian radius at t = 10 milliseconds;
• Problem M, ° Problem Herman

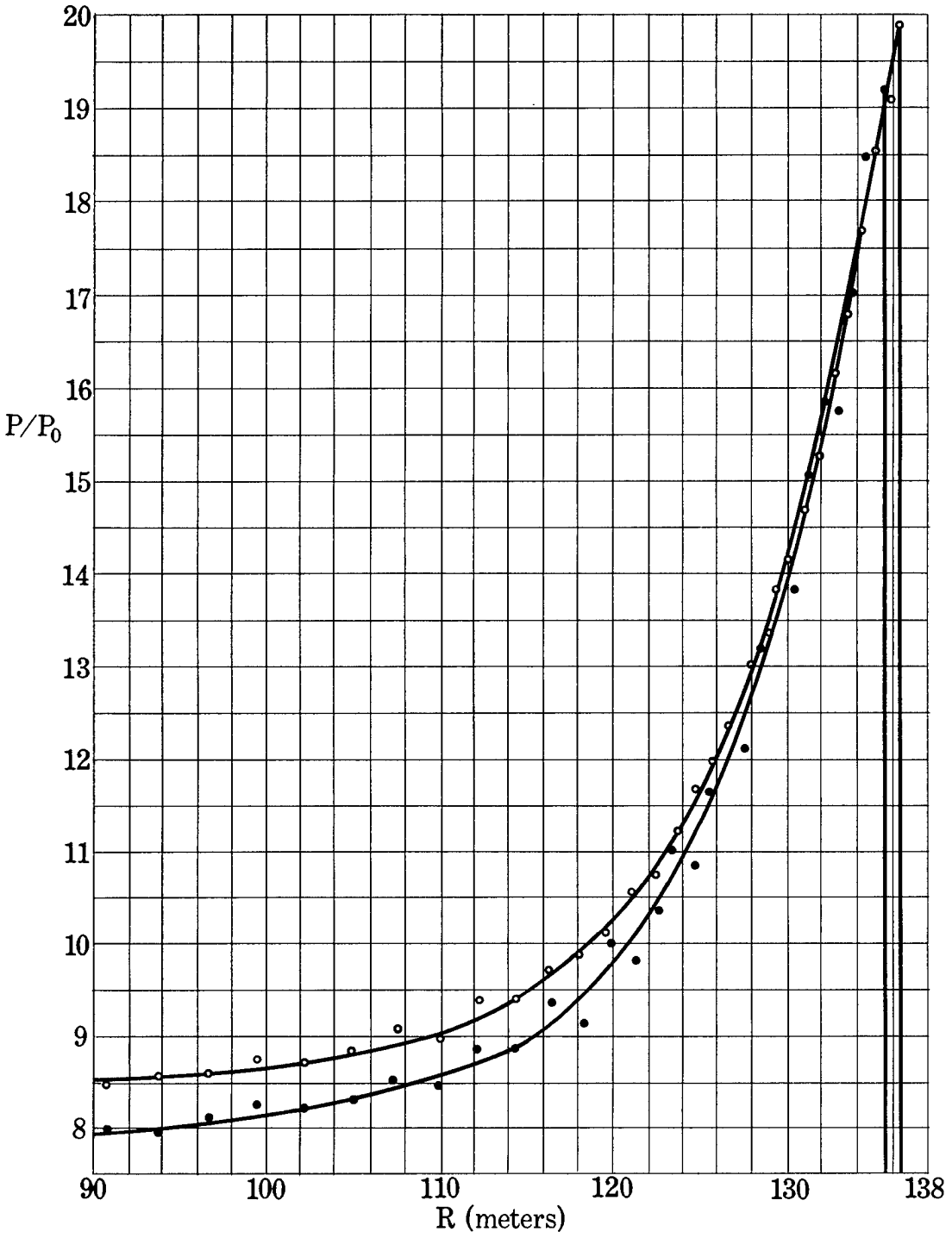

Fig. 4. Pressure as a function of the Eulerian radius at t = 30 milliseconds; • Problem M, ° Problem Herman

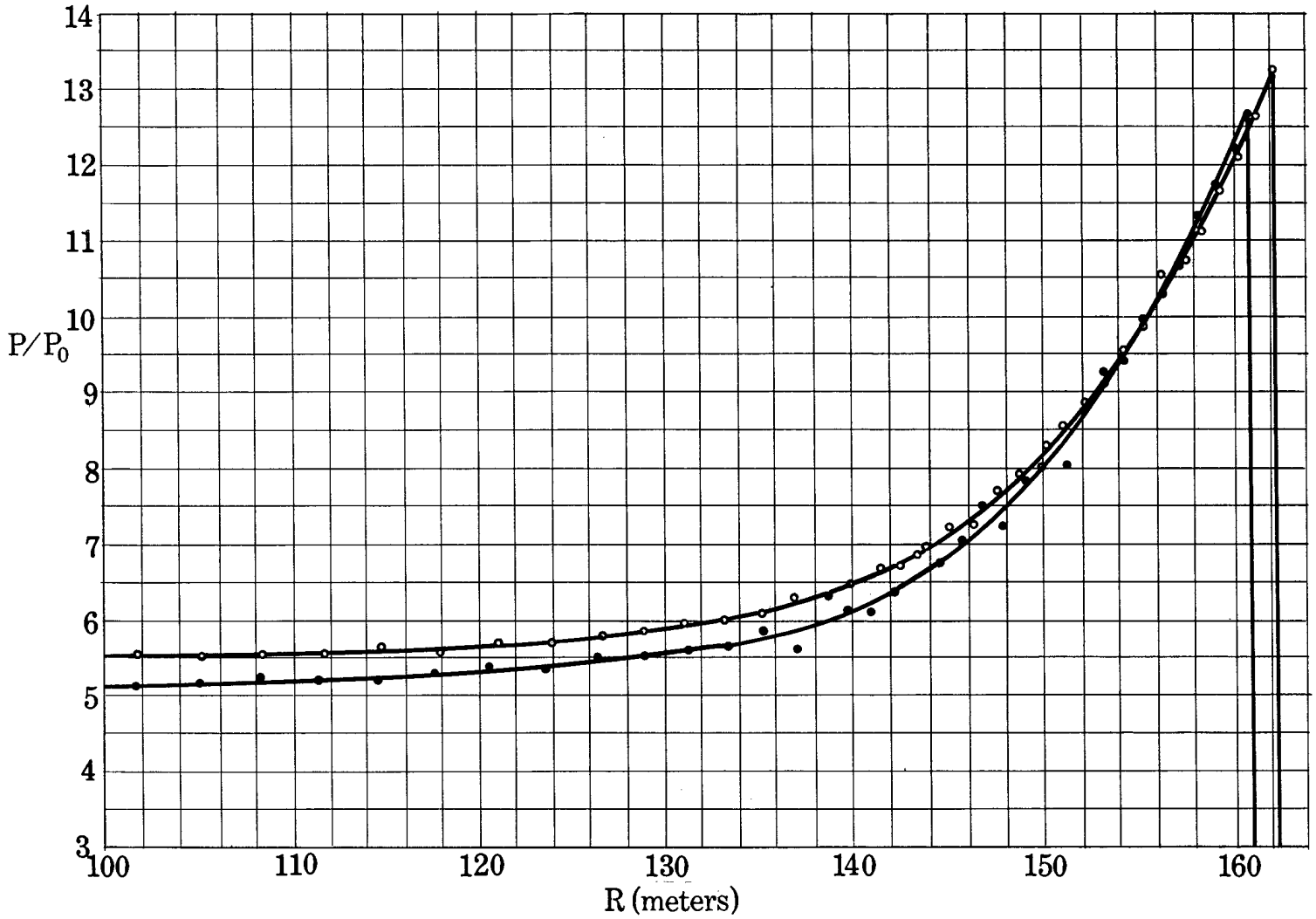

Fig. 5. Pressure as a function of the Eulerian radius at t = 50 milliseconds; • Problem M, ∘ Problem Herman

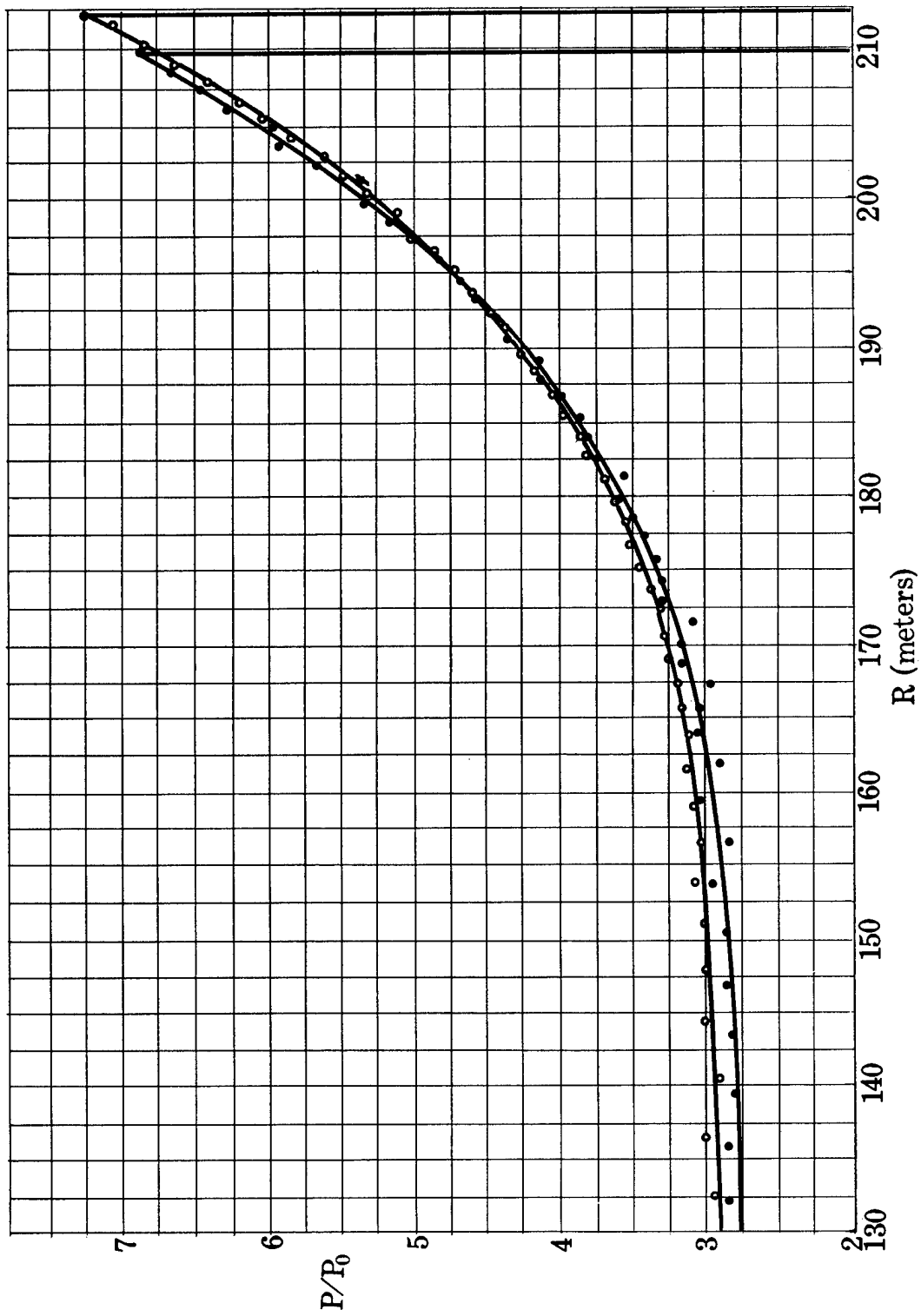

Fig. 6. Pressure as a function of the Eulerian radius at t = 100 milliseconds; • Problem M, ∘ Problem Herman

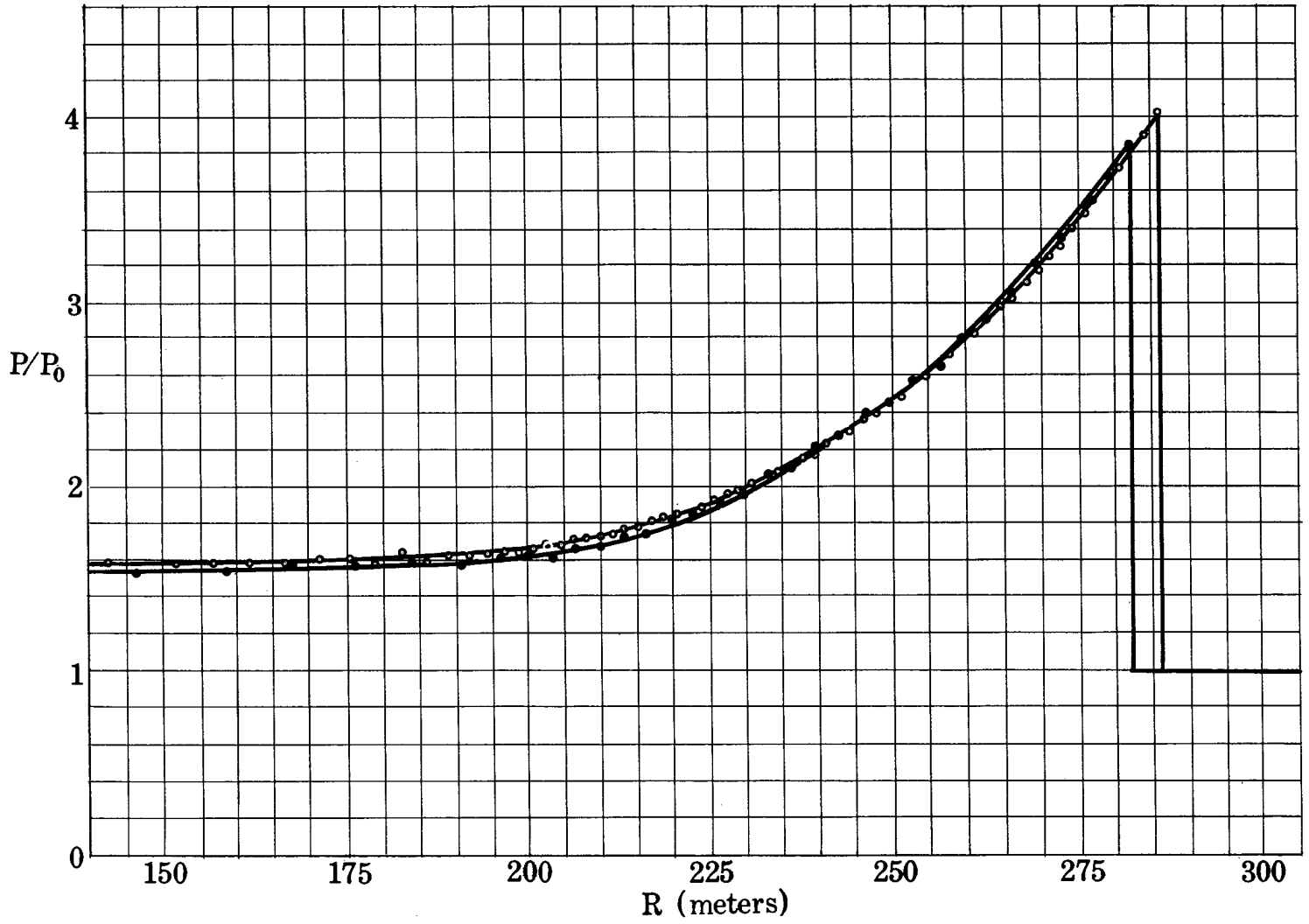

Fig. 7. Pressure as a function of the Eulerian radius at t = 200 milliseconds; • Problem M, ∘ Problem Herman

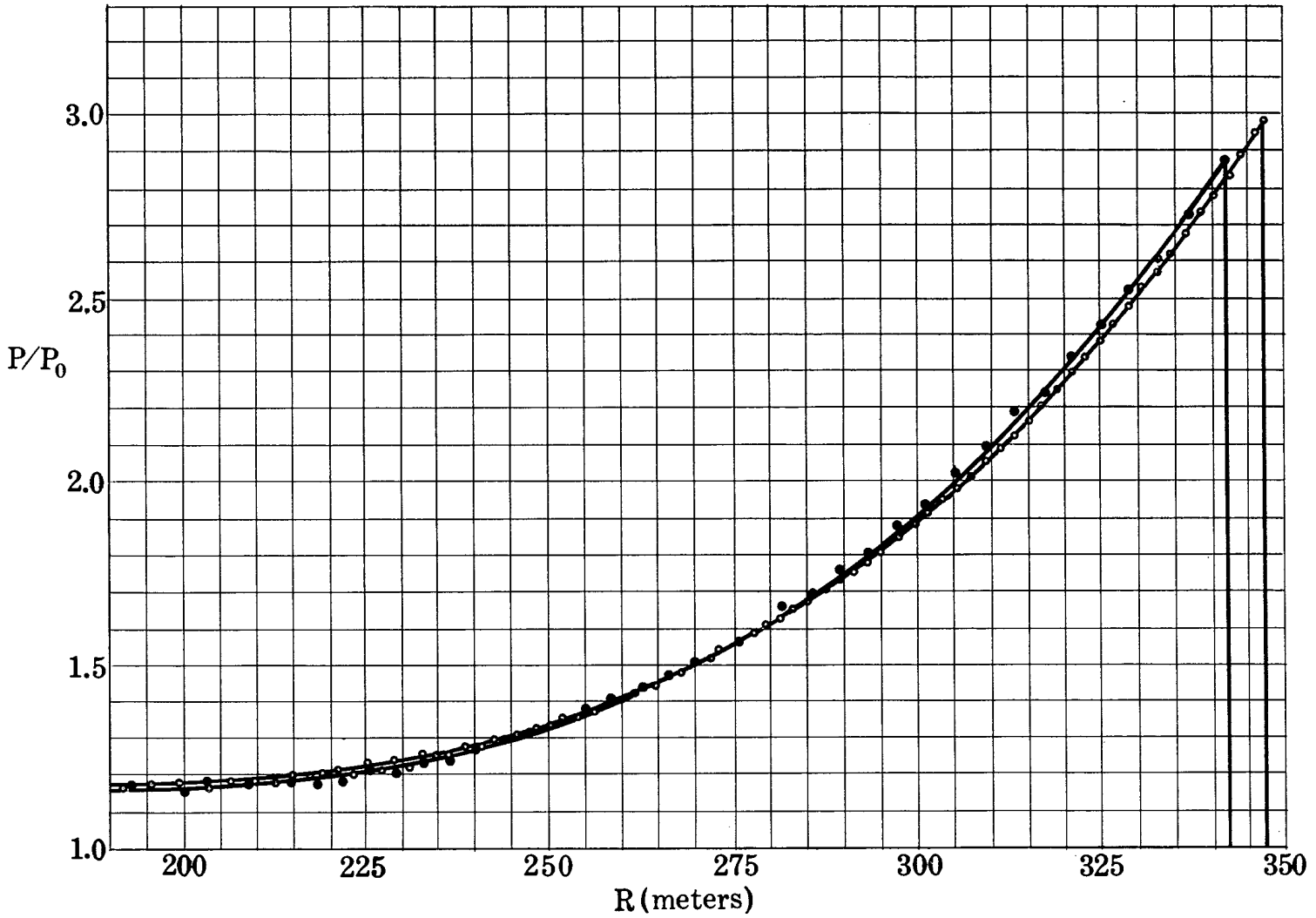

Fig. 8. Pressure as a function of the Eulerian radius at t = 300 milliseconds; • Problem M, ° Problem Herman

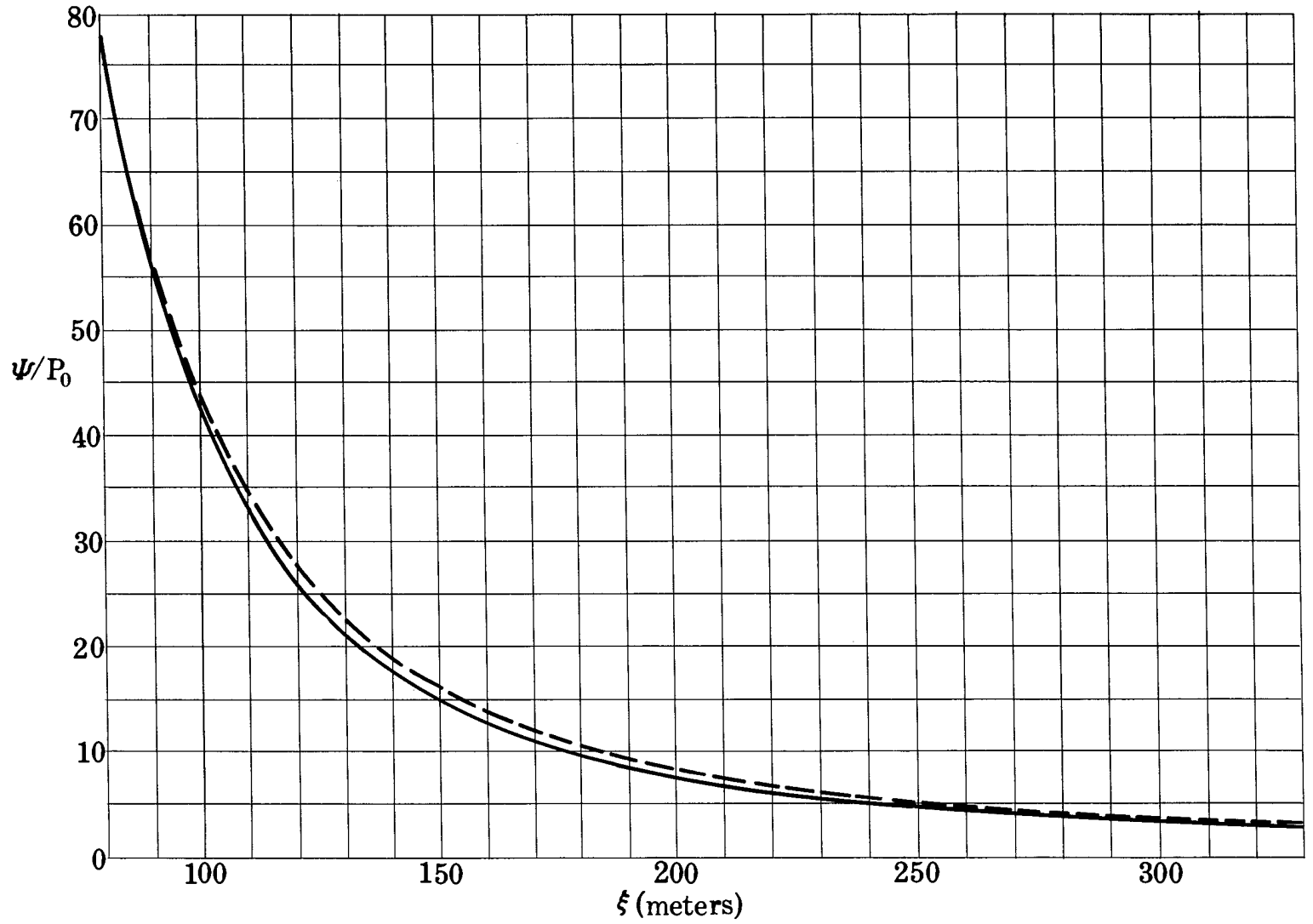

Fig. 9. Shock pressure as a function of shock position; ——— Problem M, — — — Problem Herman

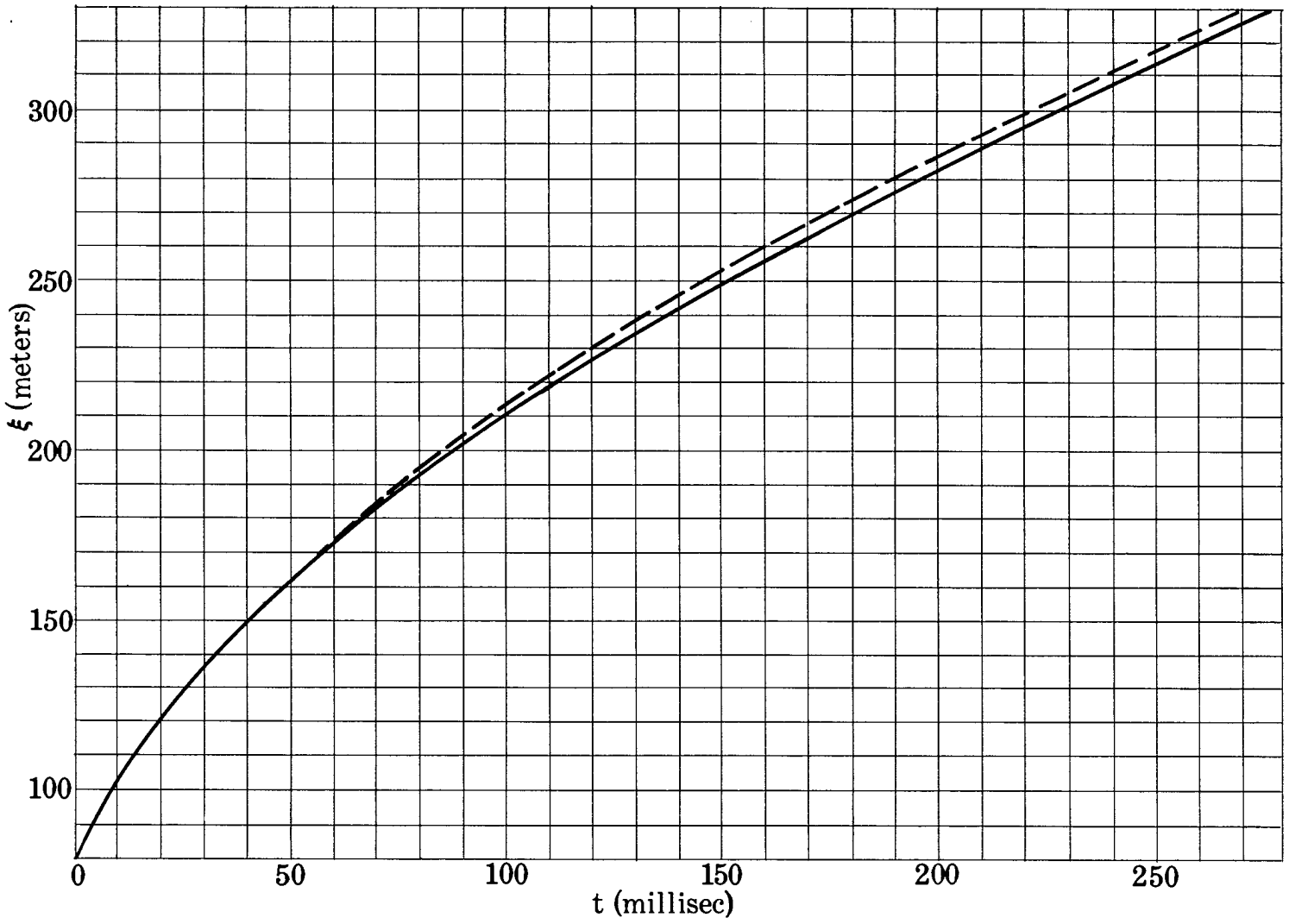

Fig. 10. Shock position as a function of time; ——— Problem M, — — — Problem Herman

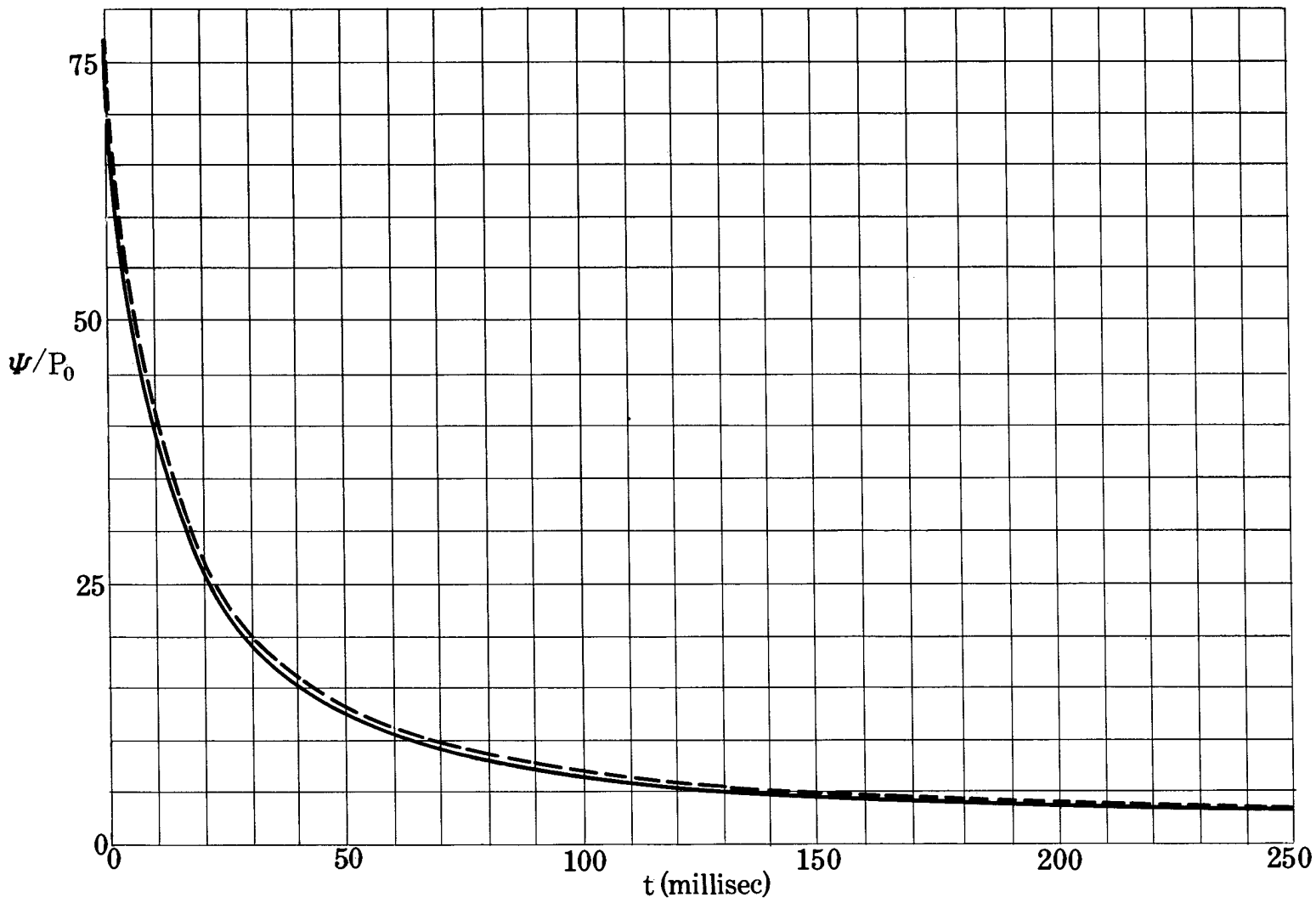

Fig. 11. Shock pressure as a function of time; ——— Problem M, — — — Problem Herman

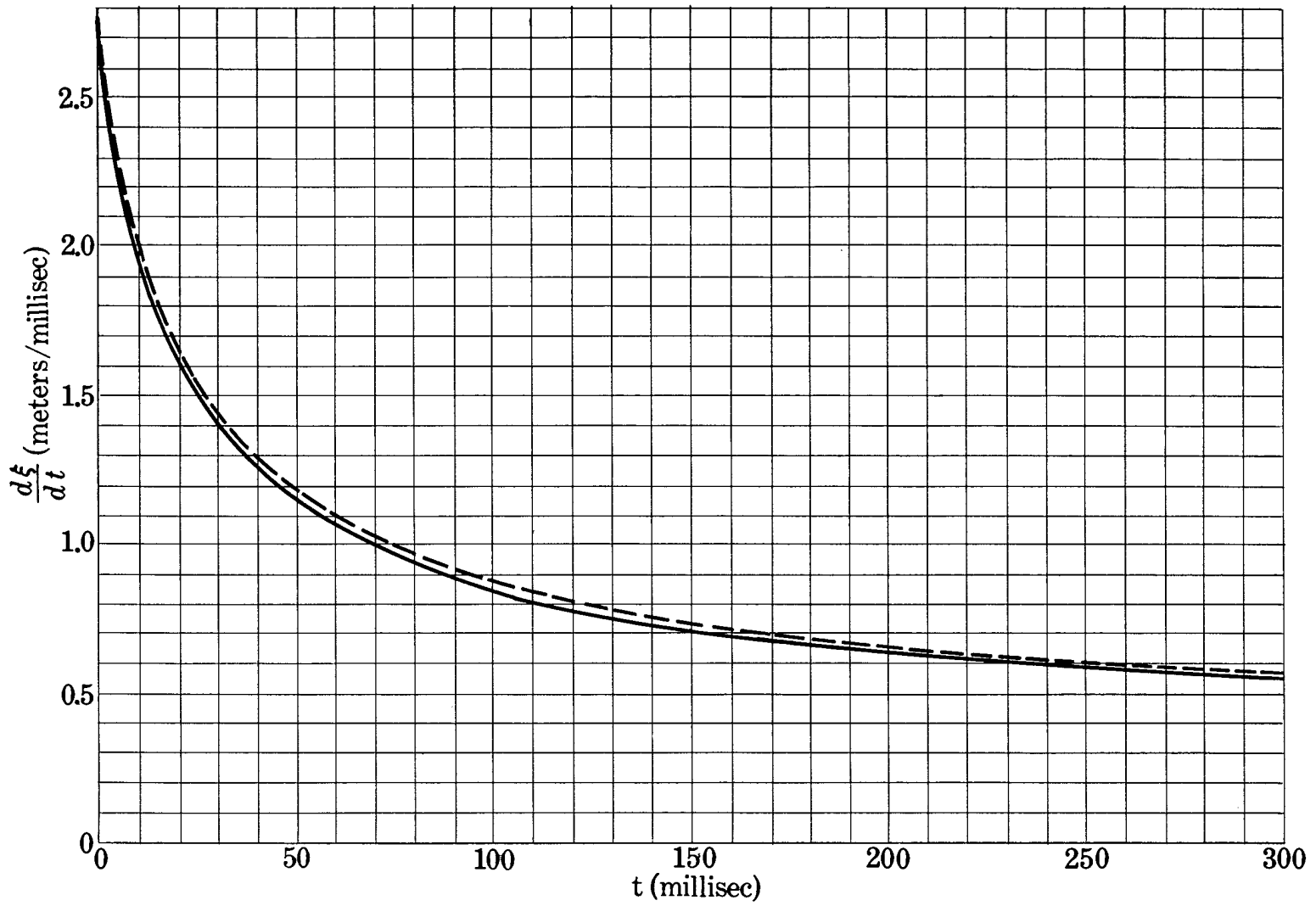

Fig. 12. Shock velocity as a function of time; ——— Problem M, — — — Problem Herman

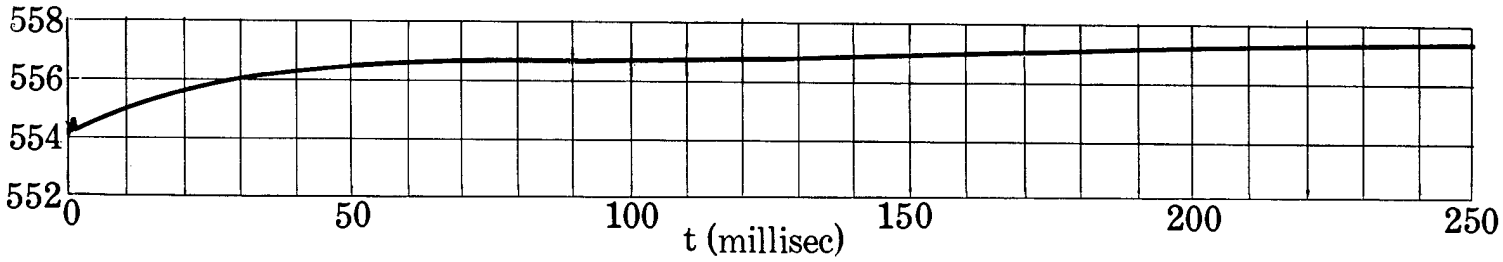

Fig. 13. Total energy as a function of time

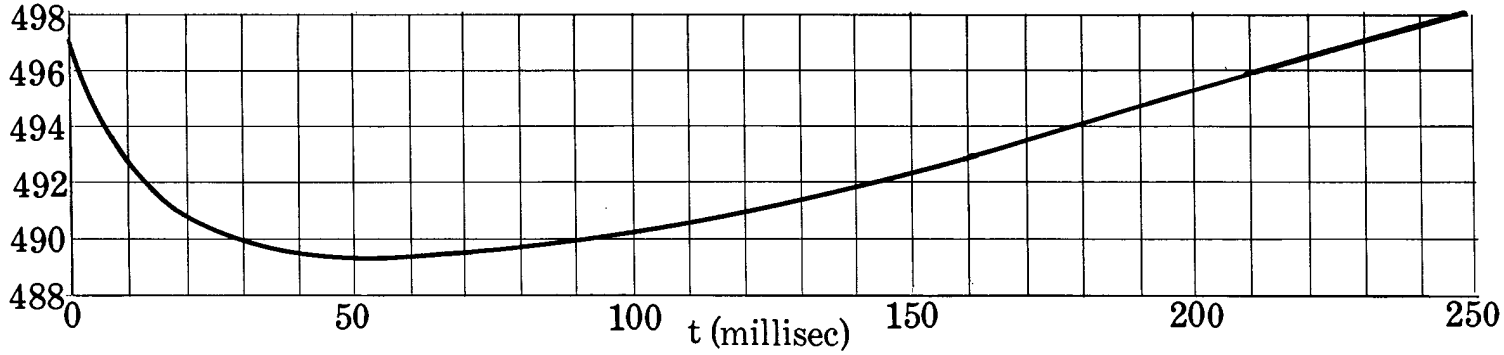

Fig. 14. Total internal energy as a function of time

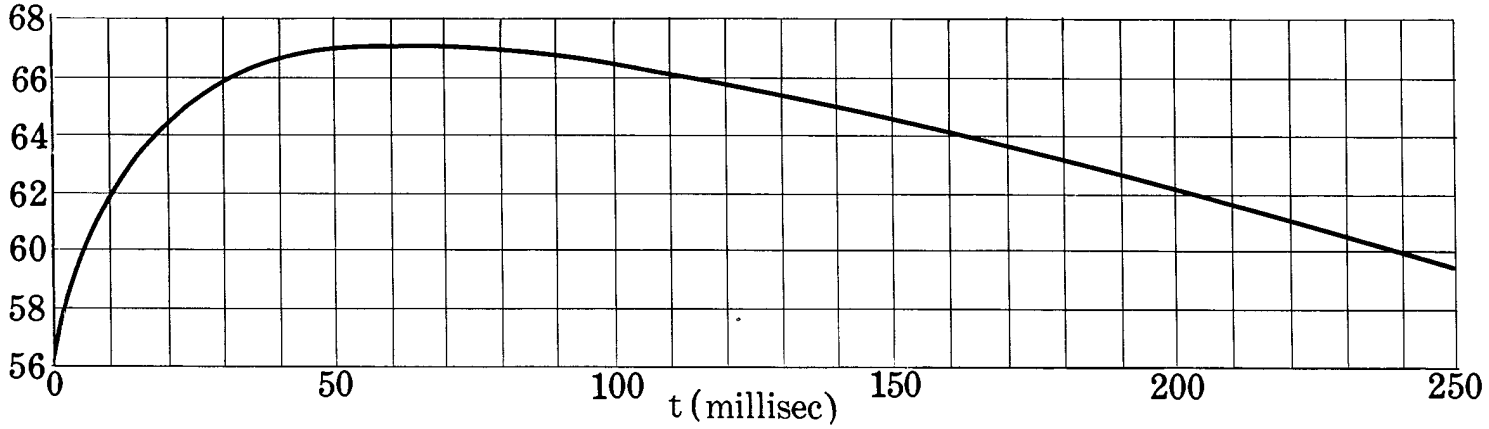

Fig. 15. Total kinetic energy as a function of time

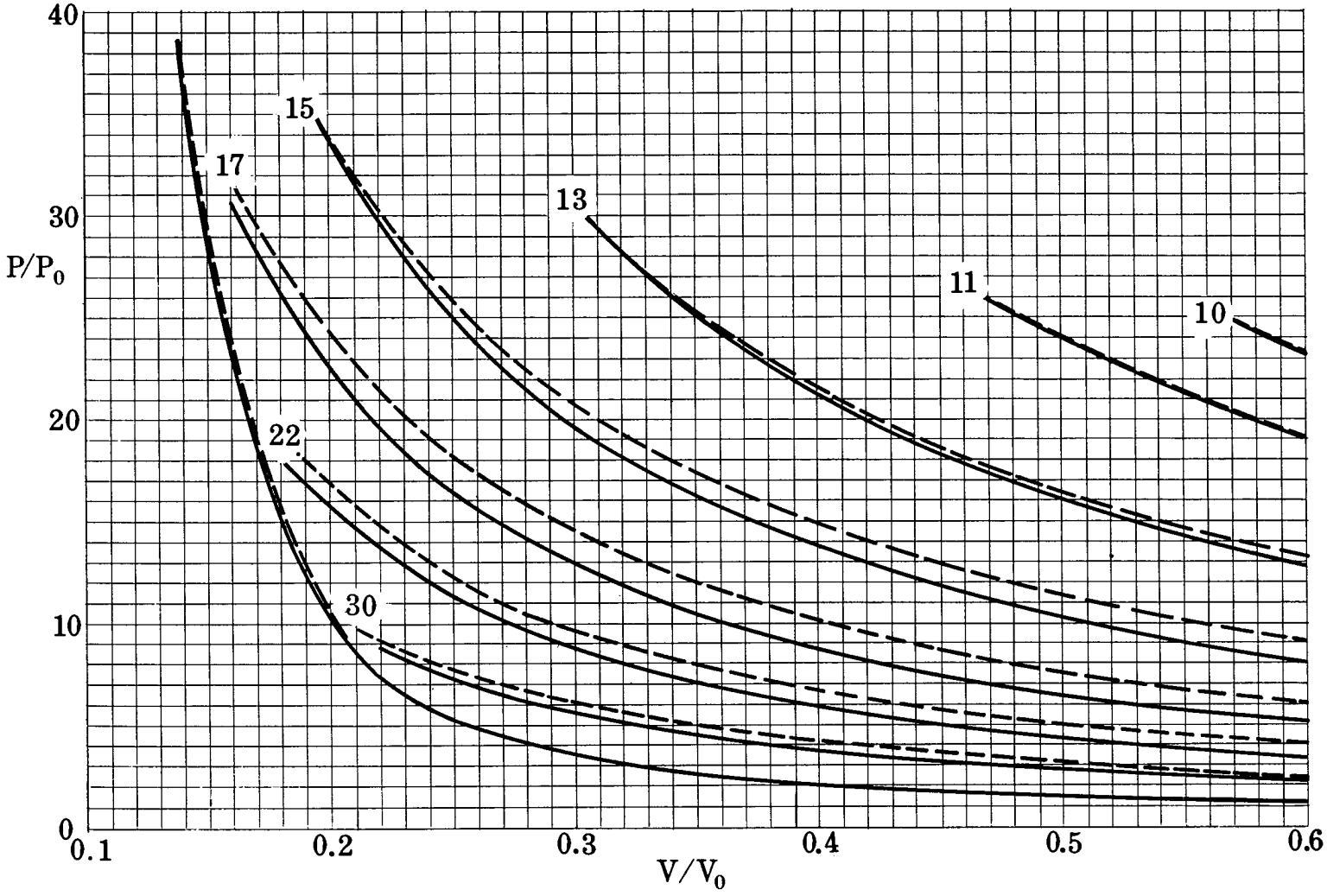

Fig. 16. The Hugoniot curve and some adiabatic curves in the pressure-volume plane;
———Problem M, — — —Problem Herman